RESEARCH PAPER

An Electrochemical Sensor Based on Nickel Oxides Nanoparticle/ Graphene Composites for Electrochemical Detection of Epinephrine

Mohammad Mazloum-Ardakani*, Fatemeh Farbod and Laleh Hosseinzadeh

Department of Chemistry, Faculty of Science, Yazd University, Yazd, Iran

ARTICLE INFO

Article History:
Received 16 July 2016
Accepted 11 September 2016
Published 1 October 2016

Keywords:
Electrocatalytic
Electrodeposition
Graphene
Nanocomposite
Nickel oxide nanoparticles

ABSTRACT

The combination of graphene and nickel oxide nanoparticles yields nanostructured electrochemical sensor formed a novel kind of structurally uniform and electrocatalytic activity material. In cyclic voltammetry studies, in the presence of epinephrine, nickel oxide / graphene composite modified electrode shows a significantly higher current response for epinephrine oxidation. Based on differential pulse voltammetry technique, the oxidation of epinephrine exhibited the dynamic range between 1.0–1800.0 μM and the detection limit was 0.42 μM. Finally, the resulting sensor was used to detect epinephrine and AC simultaneously in human serum samples.

How to cite this article
Mazloum-Ardakani M, Farbod F, Hosseinzadeh L. An Electrochemical Sensor Based on Nickel Oxides Nanoparticle/ Graphene Composites for Electrochemical Detection of Epinephrine. J Nanostruct, 2016; 6(4): 293-300. DOI: 10.22052/jns.2016.38482

INTRODUCTION

Graphene (GR), a two-dimensional honeycomb sheet of sp^2-hybridized carbon atoms, has attracted increasing attention in recent years due to its outstanding properties since its first discovery by Novoselov and Geim [1–3]. As a novel class of 2D nano-carbonaceous material, GR exhibits several of extraordinary characteristics, such as excellent thermal and electrical conductivity, high values of mechanical stiffness, and high specific surface area [4–6]. Due to the high transparency, high conductivity, high flexibility, and excellent chemical/ physical stability, GR holds great potential as window electrode materials. Additionally, GR has low price, exhibits suitable electrocatalytic activity for a variety of redox reactions, and relatively inert electrochemistry [7–9]. In view of these properties, GR has been widely used in modified electrodes for electrochemical applications.

Direct electrochemical deposition of inorganic crystals especially metal nanoparticles, on highly conductive GR-based substrates, is an attractive approach for thin film based applications [10]. The catalytic activity of metallic nanoparticles depends strongly on the shape and size, and the aggregation of these nanoparticles can decrease their catalytic activity. The suitable support for nanoparticles such as GR provides high surface area for distributing more of nanoparticles and avoids aggregation [9]. Thereby these traits result in improved catalytic, electronic, and magnetic properties of metallic nanoparticles

Recently, application of GR-based nanocomposite electrodes for biological compounds has become an interesting research topic. For example Liu et al. studied Cu_2O nanocubes, wrapped with GR nanosheets, based non-enzymatic glucose sensors. They found that the GR served as an additional surfactant during the synthesis of the nanocomposite, thereby reducing the size of the Cu_2O nanocubes and preventing particle aggregation of the Cu_2O, both of which enhanced the electrochemical stability [11]. Y. Song *et al.*

* *Corresponding Author Email: Mazloum@yazd.ac.ir*

developed a non-enzymatic amino acid sensor by electrodeposition of Co NPs on GR/GCE. They found that these homogeneous Co NPs exhibited good catalytic activity for the oxidation of cysteine and N-acetyl cysteine [12]. Metal nanoparticles possess three important potentials for electroanalysis. These include 1) the roughening of the conductive sensing interface, 2) the catalytic properties of the nanoparticles permitting their enlargement with metals and the amplified electrochemical detection of the metal deposits, and 3) the conductivity properties of nanoparticles at nanoscale dimensions that let for the electrical contact of redox centers in target molecules with electrode surfaces. Iron family metals (Fe, Co, Ni) are attracting more and more interest for their low prices and excellent performance in catalysis, such as hydrogenation [13], CO oxidation [14], alcohol oxidation [15], and electrochemistry [16]. Besides, nickel oxide (NiO) nanostructures based materials have been also widely used in supercapacitors and electrochemical sensors due to their excellent electrocatalytic and inexpensive properties [17]. However, NiONPs supported on GR nanosheets could be a nanocomposite with excellent catalytic effect.

It is very important to develop simple, sensitive and accurate methods for detecting active compounds, since drug monitoring plays an important role in drug quality control and this has a great influence on public health [18–20]. Epinephrine (EP) is a hormone and a neurotransmitter. Medically, EP has been used as a common emergency healthcare medicine. EP has an important role in a series of biological activities and nervous chemical processes [21]. Therefore, fast, easy and accurate detection of EP is important not only for detection, but also for pathological research. Several methods have been developed to determine EP such as chemiluminescence [22], capillary electrophoresis [23], spectrophotometry [24], self-assembled monolayer modified electrode [25], carbon nanotube modified electrode [26].

The present study deals with simultaneous determination of EP and AC using NiO NPs/ GR modified glassy carbon electrode. The morphological and electrochemical characterization of the electrode material has been carried out by using various techniques, such as scanning electron microscopy (SEM), cyclic voltammetry (CV), chronoamperometery (CA), and differential pulse voltammetry (DPV). This modified electrode shows good sensitivity and selectivity for determination of EP and AC in blood serum samples.

MATERIALS AND METHODS

Apparatus and chemicals

Electrochemical experiments were carried out using a computerized potentiostat/galvanostat (SAMA 500, electroanalyzer, system, I.R. Iran). A conventional three electrode cell was used. A saturated calomel electrode, a platinum wire, and a NiO/GR/GCE were used as reference, auxiliary and working electrodes, respectively. A Metrohm 691 pH/ ion meter was also used for pH measurements. All solutions were freshly prepared with double distilled water. EP and AC were of analytical grade from Sigma Aldrich. Graphite powder, NH_3, H_3PO_4, H_2O_2, ethanol, HCl, $KMnO_4$, hydrazine monohydrate (N_2H_4, 98%), sulfuric acid, $Ni(NO_3)$ and CH_3COOH were purchased from Merck.

Synthesis of graphene nanosheet

Graphene oxide (GO) was obtained by oxidizing graphite using an improved method [27]. A 9:1 mixture of concentrated H_2SO_4/H_3PO_4 (360:40 mL) was added to a mixture of graphite flakes (3.0 g) and $KMnO_4$ (18.0 g). The reaction was then heated to ~ 50 °C and stirred for 12 h. The reaction was cooled to room temperature and poured onto ice (400 mL) with 30% H_2O_2 (3 mL). The obtained solution was centrifuged, and then filtered. The solid material was then washed with distilled water until pH becomes neutral, and subsequently washed with 30% HCl and finally twice with 200 mL of ethanol. The filtered solid residue was vacuum-dried for 24 h at 40◦C. The graphite oxide was obtained as brownish yellow powder. Reduced GR oxide was synthesized using hydrazine together with ammonia solution. A colloidal suspension of GO in purified water (100 mg/100 mL) was prepared by sonication for 2 h. Then the pH of GO suspension increased to 9 by adding ammonia solution. Subsequently, 150 µL of hydrazine solution was added and then was refluxed at 85◦C for 12 h in a heating mantle and cooled to room temperature. Finally solutions were centrifuged, and GR precipitates were washed with deionized water and then dried at 60°C in vacuum for 12 h.

Preparation of NiO/GR/GC electrode

To obtain the optimized conditions for preparing NiO/GR/GCEs, we optimized the concentrations (1 mg/1mL) and volumes (1 µL) of GR suspensions and also electrodeposition time (7 s) of nickel oxides nanoparticles. GCE was carefully polished with alumina on polishing cloth, then washed with DI water, and allowed to dry under ambient condition. In order to form GR- metal NPs composite on GCE, firstly 1 µL of GR suspension (1 mg/1 mL) was casted on the bare electrode, and then permitted to dry at room temperature. Secondly, nickel oxide NPs was electrodeposited on the surface of GR/GCE from pH 4 acetate buffer solution containing 5 mM nickel nitrate, and constant potential of -1.1 V was applied for 7 seconds using chronoamperometry method. In this area, various experimental parameters including salt solution concentration, potential and time of deposition can be manipulated to control the nucleation and growth rate of the metal NPs [28]. For example longer deposition time causes the nanoparticles to aggregate into much larger particles, which could decrease the catalytic effect of NiO nanoparticles and thus negate the relative advantage of larger electroactive surface area of smaller nanoparticles. Finally, modified electrode was eventually washed with double distilled water. For comparison, GR/GCE without NiO, and NiO modified without GR, and unmodified GCE in the absence of GR and NiO were also prepared in the same way.

RESULTS AND DISCUSSION

Characterization of GR and NiO/GR

The morphology of GR and NiO electrodeposition on GR was characterized by a scanning electron microscopy (SEM). SEM image of GR (Fig.1A) exhibited morphology of wrinkling paper-like structures. In fact, GR serves as a conductive bridge and provided a wide substrate connecting the NiO nanoparticles together, which activated the NiO nanoparticles and increased the electroactive surface area (Fig.1B). The uniform distribution of high amount of NiO nanoparticles on the reduced graphene oxide nanosheet could be observed. On the other hands, the deposited surface species were constructed like a 3D structure, which increased the accessibility of analyte. IR spectroscopy (Fig.1C) indicated the presence of COOH, OH and C−O on GO sheet. The IR spectrum of GO showed a C–O stretch at 1222 cm^{-1} and OH stretch at 3500–3300 cm^{-1} as well as a C–O stretch at 1720–1690 cm^{-1} [29]. After the

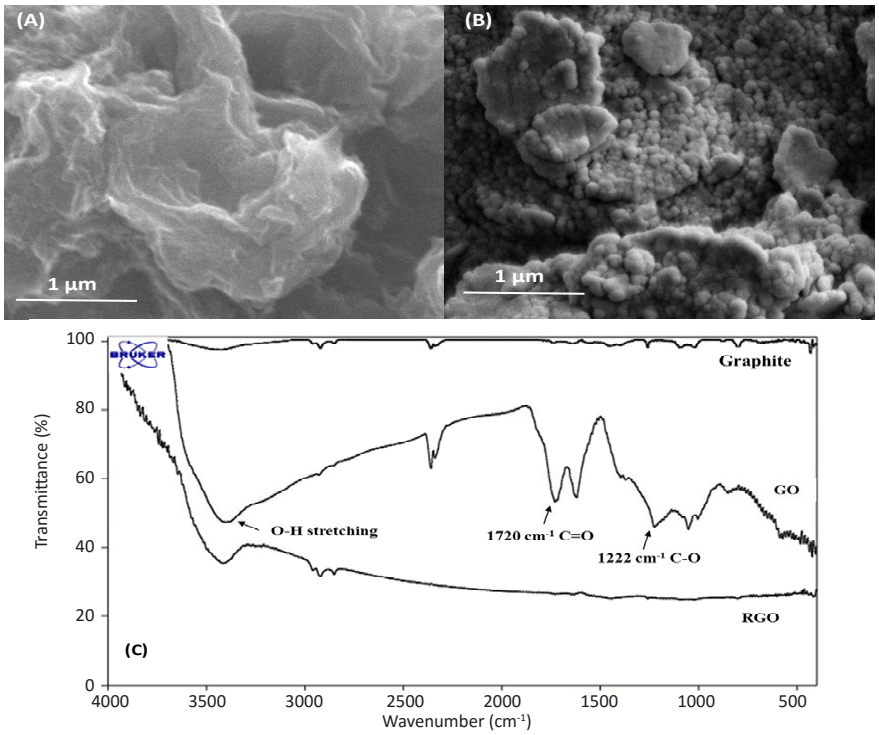

Fig. 1. SEM image of GR (A) and NiO/GR (B) and (C) FTIR spectrum

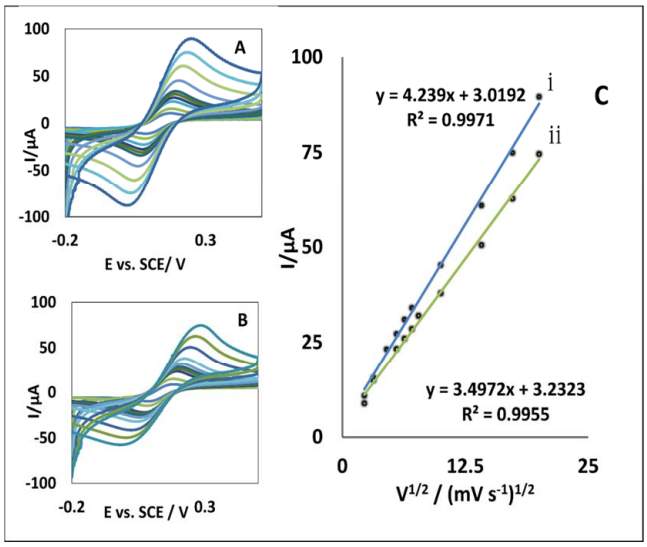

Fig. 2. CVs of NiO/GR/GCE (A) and NiO/GCE (B) in 5.0 mM $[Fe(CN)6]^{3-/4-}$ in 0.1 M KCl at various scan rates. (C) Peak current vs. square root of the scan rate for NiO/GR/GCE (I) and NiO/GCE (I I).

final reduction with hydrazine, the absence of the peaks at 1720–1690 and 1222 cm^{-1} indicated epoxide and hydroxyl groups attached to the basal GR layer have been removed (Fig. 1C).

Electrochemical properties of NiO/GR/GCE

The electrochemical effective surface area (A) of two modes of electrode including the NiO/GR/GCE and NiO/GCE were calculated by cyclic voltammetry (CV) using 5.0 mM $[Fe(CN)_6]^{3-/4-}$ redox probe prepared in 0.1 M KCl. Fig. 2 displays a series of cyclic voltammograms on the modified electrodes as a function of different scan rates and the dependence of the peak current (I_p) on the square root of the scan rate ($v^{1/2}$) for different electrode demonstrates (Fig. 2C). The CV studies have been conducted at various scan rates to investigate the interfacial kinetics on the electrodes surface. As can be observed in Fig. 2 A and B, the oxidation peak potential shifted to more positive potentials with increasing scan rate, confirming the kinetic limitation in the electrochemical reaction and the anodic and cathodic peaks of electrodes are found to move in opposite directions, suggesting the redox process to be quasi-reversible. Also, the linearity of I_p vs. $v^{1/2}$ suggested that the process is diffusion rather than surface controlled [30]. Based on the slopes of the curves of I_p vs. $v^{1/2}$ and by using Randles–Sevcik equation [30], for NiO/GR/GCE and NiO/GCE, A was calculated to be 0.038 and 0.029 cm^2 respectively. The results indicated that the electrode effective surface area was increased after modification with GR and NiO together, which would increase the adsorption capacity of Analyte, leading to enhancement of current response and increase sensitivity of sensor.

Electrocatalytic Oxidation of EP at a NiO/GR/GCE

For preparation of modified electrode, GR suspension casted on electrode surface and then NiO NPs electrodeposition, therefore, a layer of GR- NiO NPs composite formed on surface electrode which increases the conductivity of GCE greatly. Fig. 3 indicates the CV responses for the electrochemical oxidation of EP at the NiO/GR/GCE (curve d), GR modified GCE (GR/GCE) (curve c), NiO nanoparticles modified GCE (NiO/ GCE) (curve b), and bare GCE (curve a). As shown, the oxidation current of GCE, NiO/GCE, GR/GCE, NiO/GR/GCE was 12.8, 17.7, 21.1, and 31 respectively.

To investigate the roles of GR in modified electrode in the electrochemical oxidation of EP, the CVs of NiO/GR/GCE and NiO/GCE were recorded. The results indicated that the presence of GR on electrode surface exhibited 75% improvement on the oxidation peak current for EP oxidation. The evidences above seemed to suggest that NiO NPs contributed on the catalytic reaction and increase surface, also GR showed considerable catalytic feature in this case. GR gets more surface to increase the electroactive surface area, leading to more anodic peak current. The results indicated that the presence of GR and nickel oxide NPs

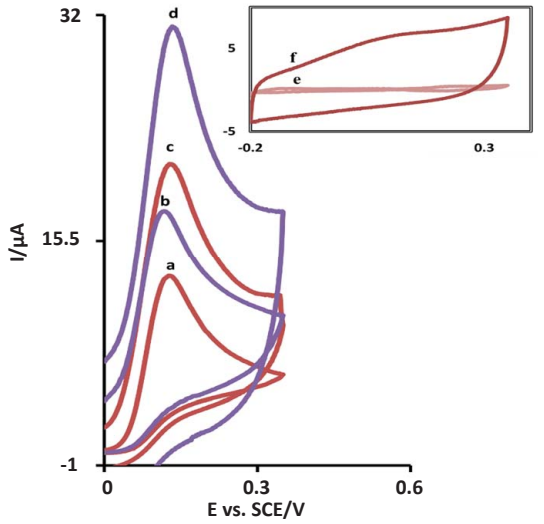

Fig. 3. CVs of (a) unmodified GCE (b) NiO/GCE (c) GR/GCE (d) NiO/GR/GCE in the presence of EP solution (pH 7.0) at a scan rate of 100 mV^{-1}. Inset: CVs of (e) unmodified GCE and (f) NiO/GR/GCE, in 0.1 M PBS (pH 7.0)

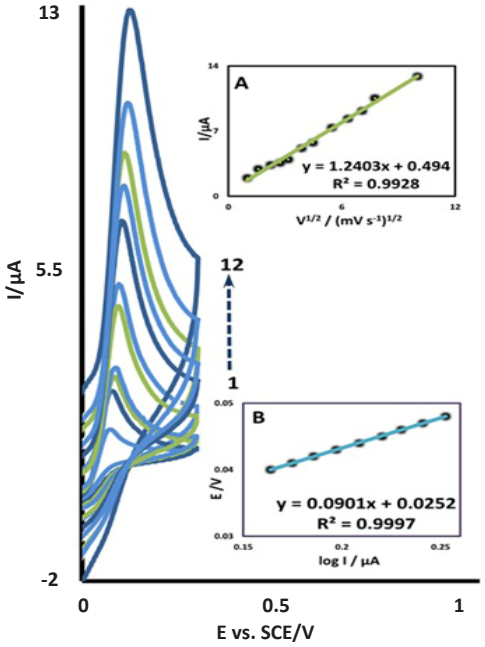

Fig. 4. CVs of NiO/GR/GCE in 0.1 M PBS (pH 7.0) in the presence of EP at various scan rates; the letters 1-12 correspond to: 5, 10, 30, 40, 50, 60, 100, 200, 300, 400 mV s^{-1}, respectively. Insets: Variation of (A) anodic peak current vs.$\upsilon^{1/2}$ and (b) Tafel plot.

together in modified electrode had great synergic effect and improved the electrochemical current response. As shown in the inset of Fig. 3, there are no redox peaks in the CVs of modified and unmodified GCE electrodes in the absence of EP at blank (PBS pH=7) solution. As expected the capacitance current value at the NiO/GR/GCE (curve f) is greater than bare GCE (curve e) which is due to the accessible capacitance of the GR at the glass carbon surface. The background current becomes too large if the concentration of the GR is higher than certain critical value.

The effect of scan rate on the electrocatalytic oxidation of EP at the NiO/GR/GCE was investigated by CV (Fig. 4). As can be seen in Fig. 4, the oxidation peak potential shifted to more positive potentials with increasing scan rate, confirming the kinetic limitation in the electrochemical reaction. Also, a plot of peak height (I_p) vs. the square root of scan rate ($v^{1/2}$) was found to be linear, suggesting that, the process was diffusion rather than surface controlled (Inset A).

A Tafel plot was drawn from data of the rising part of the voltammogram recorded at a scan rate of 20 mVs^{-1}. This part of voltammogram, known as Tafel region is affected by the electron transfer kinetics between substrate and surface-confined assuming the deprotonation of the substrate as a sufficiently fast step. In this condition, the number of electrons involved in the rate determining step can be estimated from the slope of the Tafel plot.

According to the Tafel slope equation and a slope of 0.09 V $decade^{-1}$ the charge transfer coefficient was calculated as α= 0.42 (Inset B).

Chronoamperometric Measurements

Chronoamperometry as well as other electrochemical methods was employed for the investigation of electrode processes at chemically modified electrodes. Chronoamperometric measurements of EP at NiO/GR/GCE were carried out by setting the working electrode potential at 250 mV for various concentrations of EP. For an electroactive material with a diffusion coefficient D, the current observed for the electrochemical reaction at a mass transport limited condition is described by the Cottrell equation [30]. Fig. 5 shows the fitted experimental plots for different EP concentrations. The slopes of the resulting direct lines were then plotted vs. the EP concentration (inset A). From the resulting slope and the Cottrell equation the average value of the D was found to be 6.56×10^{-5} cm^2 s^{-1}.

Chronoamperometry can also be employed to evaluate the catalytic rate constant, k'_h, for the reaction between EP and the NiO/GR/GCE corresponding to the method of Galus [31].

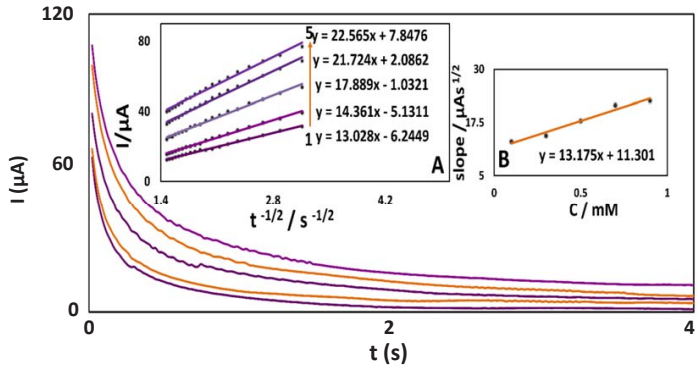

Fig. 5. Chronoamperometric obtained at NiO/GR/GCE in 0.1 M PBS (pH7.0), for different concentrations of EP. The numbers of 1–5 correspond to 0.1, 0.3, 0.5, 0.7 and 0.9 mM of EP. Insets: (A) Plots of I versus $t^{-1/2}$ obtained from chronoamperograms and (b) plot of the slopes of the straight lines against the EP concentrations.

$$I_C/I_L = \gamma^{1/2}[\pi^{1/2}\mathrm{erf}(\gamma^{1/2}) + \gamma^{-1/2}\exp(-\gamma)] \quad (1)$$

where I_C is the catalytic current of EP at the NiO/GR/GCE, I_L is the limited current in the absence of EP and $\gamma = kC_b t$ is the proof of the error function (C_b is the bulk concentration of EP). In the cases where γ exceeds 2, the error function is almost equal to 1 and hence the above Equation can be reduced to:

$$I_C/I_L = \pi^{1/2}\gamma^{1/2} = \pi^{1/2}(kC_b t)^{1/2} \quad (2)$$

where t is the time elapsed. The above equation can be used to calculate the rate constant, k, of the catalytic process from the slope of the I_C/I_L vs. $t^{1/2}$ at a given EP concentration (inset B). From the values of the slopes, the mean value of k was found to be 8.7 M^{-1} s^{-1}.

Differential pulse voltammetry investigations

Differential pulse voltammetry (DPV) has the advantage of an increase in sensitivity and better characteristics for analytical applications. DPVs for the oxidation of different concentrations of EP at the NiO/GR/GCE were obtained (Fig. 6). Voltammograms clearly show that the plot of peak current versus EP concentration is constituted of two linear segments with different slopes (slope: 0.1075 μA.μM^{-1} for first linear segment and 0.0254 μA.μM^{-1} for second linear segment), corresponding to two different ranges of substrate concentration (1 to 100 μM for first linear segment and 100 to 1800.0 μM for second linear segment). The decrease of sensitivity (slope) in the second linear range is likely to be due to kinetic limitation [30]. The detection limit (3σ) for EP in the lower range region was found to be 0.42 μM.

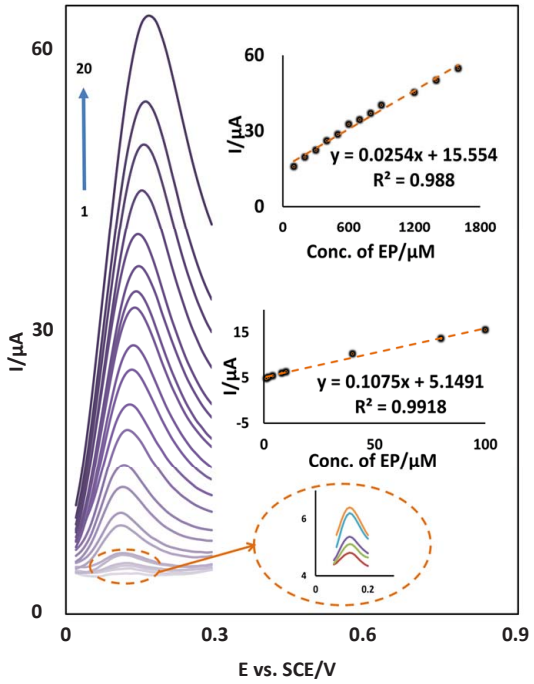

Fig. 6. DPVs of NiO/GR/GCE in 0.1 M PBS (pH 7.0) containing different concentrations of EP. The numbers of 1–20 correspond to: 1, 2, 4, 8, 10, 20, 40, 60, 100, 200, 300, 400, 600, 700, 800, 900, 1200, 1400, 1600 and 1800 μM of EP. Insets show the plot of the electrocatalytic peak current as a function of EP concentration in the ranges of 1–100 μM and 100-1800 μM.

Simultaneous Determination of EP and AC

One of the main objectives of this study was utilizing a modified electrode capable of electrocatalytic oxidation of EP and separation of the electrochemical responses of EP and AC. By using NiO/GR/GCE as a working electrode, the analytical experiments were carried out by both varying the EP and AC concentrations in 0.1 M PBS

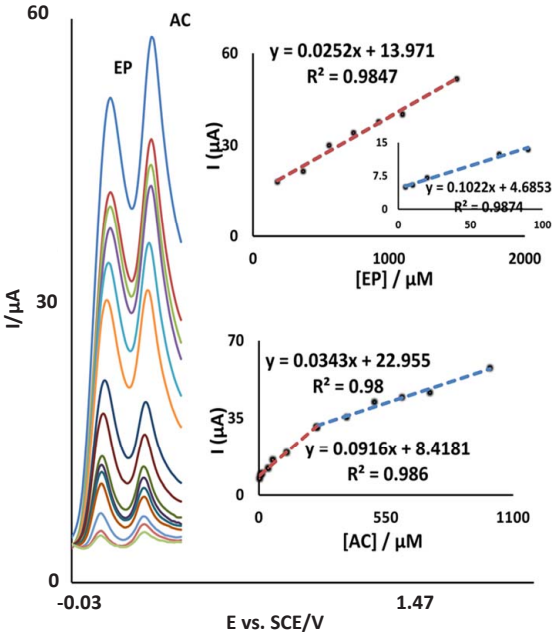

Fig. 7. DPVs of NiO/GR/GCE in a 0.1M PBS (pH 7.0) containing different concentrations of EP and AC. (from inner to outer) mixed solutions of 5 + 3, 10 + 7, 20 + 13, 70 + 40, 90 + 60, 180 + 120, 370 + 250, 550 + 400, 750 + 500, 920 + 620, 1100 + 750 and 1500 + 1000, respectively, in which the first value is the EP concentration (µM) and the second value is the AC concentration (µM). Insets: (A and B) Plots of the peak currents as a function of EP concentration and (C) plot of the peak currents as a function of AC concentration.

(pH 7.0) and recording the DPVs. The voltammetric results show that the simultaneous determination of EP and AC with well-distinguished two anodic peaks at potentials of 130 mV and 300 mV (by DPV technique), corresponding to the oxidation EP and AC, respectively, could be possible at the NiO/GR/GCE (Fig. 7). The DPV voltammograms clearly show that the plot of peak current vs. AC concentration is linear for 5-250 µM of AC. Detection limits were determined as 0.42 µM EP and 0.98 µM AC. It is very interesting to note that the sensitivities of the modified electrode towards EP in the absence and presence of AC are virtually the same. It can be noted from these results that the responses to EP and AC at the NiO/GR/GCE are relatively independent and the utilization of the NiO/GR/GCE for the simultaneous measurements of the two analytes are possible without any interference.

CONCLUSION

In summary, the nickel oxide nanoparticle film was formed electrochemically on GR in a regime of chronoamperometry on a glassy carbon electrode and tested for electro-oxidation of epinephrine. NiO/GR composite exhibits a higher capacitance compared with NiO, which is due to the special structure of the composite and good contact between active materials and GR substrates. DPV investigation showed simultaneous determination of EP and AC, with complete resolution of their anodic peaks is possible by the modified electrode. High sensitivity and selectivity of the voltammetric responses, and low detection limit, together with the ease of preparation, make the proposed modified electrode very useful for accurate determination of EP and AC in real samples.

ACKNOWLEDGEMENTS

The authors wish to thank the Yazd University Research Council, the IUT Research Council and Excellence in Sensors for financial support of this research.

CONFLICT OF INTEREST

The authors declare that there is no conflict of interests regarding the publicaton of this manuscript.

REFERENCES

1. Bello A, Fabiane M, Dodoo-Arhin D, Ozoemena KI, Manyala N. Silver nanoparticles decorated on a three-dimensional graphene scaffold for electrochemical applications. J Phys Chem Solids. 2014;75(1):109–14.
2. Novoselov KS, Geim AK, Morozov S V, Jiang D, Zhang Y, Dubonos SV and, et al. Electric field effect in atomically thin carbon films. Science. 2004;306(5696):666–9.
3. Li D, Müller MB, Gilje S, Kaner RB, Wallace GG. Processable aqueous dispersions of graphene nanosheets. Nat Nanotechnol. 2008;3(2):101–5.
4. Balandin AA, Ghosh S, Bao W, Calizo I, Teweldebrhan D, Miao F, et al. Superior thermal conductivity of single-layer graphene. Nano Lett. 2008;8(3):902–7.
5. Bolotin KI, Sikes KJ, Jiang Z, Klima M, Fudenberg G, Hone J, et al. Ultrahigh electron mobility in suspended graphene. Solid State Commun. 2008;146(9):351–5.
6. Jin Y, Jia M, Zhang M, Wen Q. Preparation of stable aqueous dispersion of graphene nanosheets and their electrochemical capacitive properties. Appl Surf Sci. 2013;264:787–93.
7. Behpour M, Meshki M, Masoum S. Study and electrochemical determination of tyrosine at graphene nanosheets composite film modified glassy carbon electrode. J Nanostruct. 2013;3(2):243–51.
8. Mazloum-Ardakani M, Khoshroo A, Hosseinzadeh L. Application of graphene to modified ionic liquid graphite composite and its enhanced electrochemical catalysis properties for levodopa oxidation. Sensors Actuators B Chem. 2014;204:282–8.
9. Mazloum-Ardakani M, Hosseinzadeh L, Taleat Z. Synthesis

and electrocatalytic effect of Ag@Pt core–shell nanoparticles supported on reduced graphene oxide for sensitive and simple label-free electrochemical aptasensor. Biosens Bioelectron. 2015 Dec 15;74(0):30–6.
10. Wang R, Lang J, Zhang P, Lin Z, Yan X. Fast and Large Lithium Storage in 3D Porous VN Nanowires–Graphene Composite as a Superior Anode Toward High-Performance Hybrid Supercapacitors. Adv Funct Mater. 2015;25(15):2270–8.
11. Liu M, Liu R, Chen W. Graphene wrapped Cu_2O nanocubes: non-enzymatic electrochemical sensors for the detection of glucose and hydrogen peroxide with enhanced stability. Biosens Bioelectron. 2013;45:206–12.
12. Song Y, He Z, Zhu H, Hou H, Wang L. Electrochemical and electrocatalytic properties of cobalt nanoparticles deposited on graphene modified glassy carbon electrode: Application to some amino acids detection. Electrochim Acta. 2011;58:757–63.
13. Rangheard C, de Julián Fernández C, Phua P-H, Hoorn J, Lefort L, de Vries JG. At the frontier between heterogeneous and homogeneous catalysis: hydrogenation of olefins and alkynes with soluble iron nanoparticles. Dalt Trans. 2010;39(36):8464–71.
14. Li L, Wang A, Qiao B, Lin J, Huang Y, Wang X, et al. Origin of the high activity of Au/FeO_x for low-temperature CO oxidation: Direct evidence for a redox mechanism. J Catal. 2013;299:90–100.
15. Zhu J, Kailasam K, Fischer A, Thomas A. Supported cobalt oxide nanoparticles as catalyst for aerobic oxidation of alcohols in liquid phase. ACS Catal. 2011;1(4):342–7.
16. Bhakta AK, Mascarenhas RJ, D'Souza OJ, Satpati AK, Detriche S, Mekhalif Z, et al. Iron nanoparticles decorated multi-wall carbon nanotubes modified carbon paste electrode as an electrochemical sensor for the simultaneous determination of uric acid in the presence of ascorbic acid, dopamine and l-tyrosine. Mater Sci Eng C. 2015 Dec 1;57:328–37.
17. Yuan B, Xu C, Liu L, Zhang Q, Ji S, Pi L, et al. Cu_2O/NiO_x/ graphene oxide modified glassy carbon electrode for the enhanced electrochemical oxidation of reduced glutathione and nonenzyme glucose sensor. Electrochim Acta. 2013;104:78–83.
18. Mazloum-Ardakani M, Hosseinzadeh L, Khoshroo A, Naeimi H, Moradian M. Simultaneous Determination of Isoproterenol, Acetaminophen and Folic Acid Using a Novel Nanostructure-Based Electrochemical Sensor. Electroanalysis. 2014;26(2):275–84.
19. Mazloum-Ardakani M, Khoshroo A. High performance electrochemical sensor based on fullerene-functionalized carbon nanotubes/Ionic liquid: Determination of some catecholamines. Electrochem commun. 2014;42(0):9–12.
20. Mazloum-Ardakani M, Khoshroo A. Synthesis of TiO_2 Nanoparticle and its Application to Graphite Composite Electrode for Hydroxylamine Oxidation. J Nanostruct. 2013;3:269–75.
21. Banks WA. The blood–brain barrier as a regulatory interface in the gut–brain axes. Physiol Behav. 2006;89(4):472–6.
22. Du J, Shen L, Lu J. Flow injection chemiluminescence determination of epinephrine using epinephrine-imprinted polymer as recognition material. Anal Chim Acta. 2003;489(2):183–9.
23. Wang A-J, Xu J-J, Zhang Q, Chen H-Y. The use of poly (dimethylsiloxane) surface modification with gold nanoparticles for the microchip electrophoresis. Talanta. 2006;69(1):210–5.
24. Bulatov A V, Petrova A V, Vishnikin AB, Moskvin AL, Moskvin LN. Stepwise injection spectrophotometric determination of epinephrine. Talanta. 2012;96:62–7.
25. Wang L, Bai J, Huang P, Wang H, Zhang L, Zhao Y. Self-assembly of gold nanoparticles for the voltammetric sensing of epinephrine. Electrochem commun. 2006;8(6):1035–40.
26. Mazloum-Ardakani M, Ahmadi SH, Mahmoudabadi ZS, Khoshroo A, Heydar KT. Electrochemical and catalytic investigations of epinephrine, acetaminophen and folic acid at the surface of titanium dioxide nanoparticle-modified carbon paste electrode. Ionics. 2014;20(12):1757–65.
27. Marcano DC, Kosynkin D V, Berlin JM, Sinitskii A, Sun Z, Slesarev A, et al. Improved synthesis of graphene oxide. ACS Nano. 2010;4(8):4806–14.
28. Huang X, Yin Z, Wu S, Qi X, He Q, Zhang Q, et al. Graphene-based materials: synthesis, characterization, properties, and applications. Small. 2011;7(14):1876–902.
29. Lomeda JR, Doyle CD, Kosynkin D V, Hwang W-F, Tour JM. Diazonium functionalization of surfactant-wrapped chemically converted graphene sheets. J Am Chem Soc. 2008;130(48):16201–6.
30. Bard AJ, Faulkner LR. Electrochemical Methods: Fundamentals and Applications. 2nd ed. Wiley; 2000.
31. Galus Z, Reynolds GF, Marcinkiewicz S. Fundamentals of electrochemical analysis. Vol. 328. Ellis Horwood New York; 1976.